Frequency Response of Microcantilevers in Supercritical CO_2

Erdal Uzunlar[1], M. Salih Kılıç[2], B. Erdem Alaca[2], Hakan Ürey[3], Can Erkey[1,*]
[1]Department of Chemical and Biological Engineering, Koç University, Istanbul, Turkey
[2] Department of Mechanical Engineering, Koç University, Istanbul, Turkey
[3] Department of Electrical and Electronics Engineering, Koç University, Istanbul, Turkey

Koç University, Rumelifeneri Yolu, 34450,
Sariyer, Istanbul, Turkey

* cerkey@ku.edu.tr
Koç University, Rumelifeneri Yolu, 34450,
Sariyer, Istanbul, Turkey
College of Engineering,
1st floor, Office 108, Lab 105
Tel: +90 (212) 338 1866
Fax: +90 (212) 338 1548

The frequency response of microcantilevers (MCs) in supercritical CO_2 ($scCO_2$) is investigated. Nickel MCs that were 120 μm and 180 μm long, 12 μm wide and 2.5 μm thick were prepared by microfabrication techniques. The MCs and an electromagnetic actuator consisting of a copper wire wrapped around a coil were subsequently placed in a custom made Teflon housing which could fit snuggly into a 50 ml pressure vessel equipped with sapphire windows. The resonance spectra under electromagnetic actuation in $scCO_2$ was measured using a Laser Doppler Vibrometer (LDV) in the pressure range of 1200-2000 psig with 100 psig intervals and at a temperature of 33.6 °C. The resonance frequencies were found to vary linearly both with density and viscosity, thus with kinematic viscosity. However, the relationship between the quality factors and kinematic viscosity was found to depict a highly nonlinear character. Added mass analysis was performed using the first order Taylor series expansion of the resonance frequency expression written as a function of added mass caused by pressure load for a case where viscous drag is neglected. It was seen that the mass resolution of both MCs is almost on the order of nanograms. The extrapolation of resonance frequency versus density, resonance frequency versus viscosity (dynamic) and resonance frequency versus kinematic viscosity lines enabled the calculation of vacuum frequency of the MCs with an average percentage error of 1.7 %, 10.1 % and 4.6 %, respectively. In addition, a linear relationship between the damping coefficient and the square root of viscosity was observed with an R^2 value of 0.9645 only for 180 μm long cantilevers which enabled us to calculate viscosity of $scCO_2$ with a percentage error less than 5 %. This result could also be combined with the linear behavior of resonance frequency versus kinematic viscosity curves to calculate density of $scCO_2$ with a percentage error less than 3 %.

INTRODUCTION

Micromechanical resonators have been extensively studied in recent years because of their potential for high-sensitive, low cost, compact device applications, such as mass sensors [1, 2], force sensors [3], viscometers and densitometers [4-12], chemical [2, 13, 14] and biological [1] sensors, explosive detectors [2], devices for mechanical characterization (e.g. for determining Young's modulus) [15] and for studying microscale phenomena (e.g. Knudsen effect) [16]. The dynamics of microcantilevers (MCs) in fluids are important in the atomic force microscopy in biological buffers [5], naval architectural design [17] and the design of aforementioned viscometers and densitometers. In the operation of MCs in a fluid, viscosity and density of the fluid are crucial parameters since the hydrodynamic length scale of the MCs are comparable to the viscous penetration depth in the fluid [18].

The behavior of the MCs immersed in fluids is mostly investigated by the changes in the resonance spectra, i.e. the shifts in the resonance frequency, f_R, and the quality factor, Q. f_R corresponds to the frequency at which the maximum amplitude of oscillation is achieved and the Q is the measure of sharpness of the resonance peak formulated as $Q=f_R/2g$, in which the frequencies f_R+g and f_R-g above and below f_R at which the amplitude is equal to $A_{max}/2^{1/2}$, where A_{max} is the maximum amplitude of oscillation achieved at f_R [10]. The resonance spectra, i.e. amplitude versus frequency, can be extracted in a discrete manner by first a frequency sweep and then a Lorentzian function fit that can be found elsewhere or in a continuous manner by Fast Fourier Transform (FFT) as power or thermal spectra. A representative Lorentzian function fit to the resonance spectra of the fundamental flexural mode of vibration with normalized amplitude using MATLAB can be seen in Figure 1.

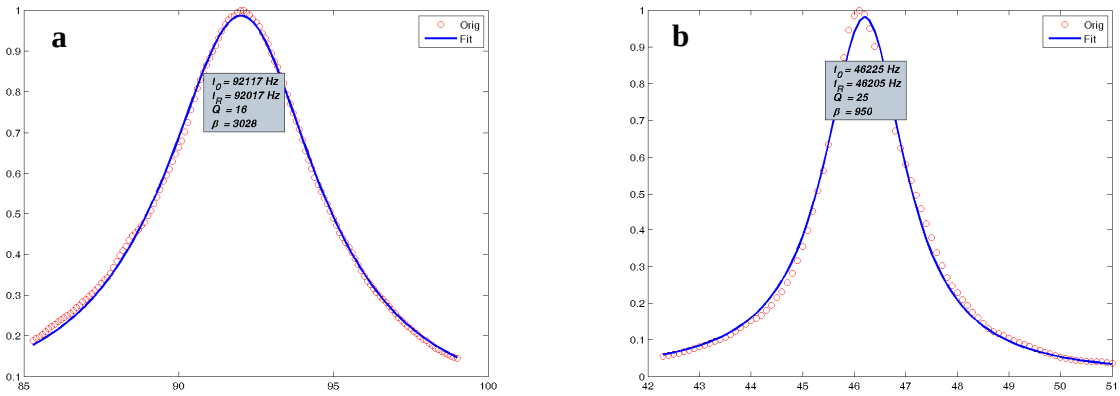

Figure 1: Representative Lorentzian fit to the obtained resonance spectra taken from Ni cantilevers of sizes (width x length x thickness, in μm) (a) 12x120x2.5 (b) 12x180x2.5

When a MC is placed in a fluid (liquid or gas), the resonance frequency and quality factor decreases with increasing density and viscosity of the fluid. This phenomenon can be explained by two naive approximations where the effects of density and viscosity are assumed to be decoupled. First, the resonance frequency decreases with increasing density due to added mass, a phenomenon which is considered as inertial effect. Second, the quality factor decreases with

increasing viscosity, i.e. the broadening of the resonance peaks, because of the shearing motion at the tip of the MC which acts as a damping to the oscillations, another phenomenon which is known as dissipative effects [10]. However, in the actual case, the effects of density and viscosity on the dynamics of MCs are coupled and the complex behavior is described by the hydrodynamic function by which the inertial and dissipative effects are quantified [4].

In this study, we investigated the frequency response of MCs in supercritical CO_2 ($scCO_2$) in the pressure range of 1200-2000 psig with approximately 100 psig intervals at a temperature of 33.7 °C. Nickel MCs with dimensions of (width x length x thickness) 12x120x2.5 and 12x180x2.5 were fabricated by the conventional microfabrication techniques. A custom made Teflon housing was used to mount the MCs and an electromagnetic actuator into a 50 ml pressure vessel containing two sapphire windows. An optical read-out system consisting of a Laser Doppler Vibrometer (LDV) and GPIB-USB interface was used to measure the resonance spectra. The acquired frequency response was fitted by a Lorentzian function from which the resonance frequency, quality factor and damping coefficient were extracted.

MATERIALS AND METHODS

For the fabrication of Ni MCs, first a 500 μm thick 4 inches SOI wafer on which a thin layer of Cr and Au had been sputtered was spin-coated with a photoresist. Then, photolithography was performed using the related mask. After the development of the pattern was developed, the wafer was divided into 1 cm x 1 cm chips. Ni electroplating was conducted for each chip, and the photoresist was then removed. Finally, the Cr and Au layers were wet-etched. The resulting profile and surface quality of the cantilevers are observed by an optical microscope.
A vibration-free tabletop was prepared by using 4 Thorlabs PWA071 Passive Isolation Mounts placed under a granite block. On top of the block, a Polytech OFV-2500 LDV and a 50 ml TharSFC 05424-4 view cell were fixed on a 30 cm x 45 cm breadboard. The LDV camera was connected a 15 inches screen CRT TV. CO_2 was supplied from Messer Aligaz with an indicated purity of 99.9% by volume and pumped using a TELEDYNE ISCO D Series Pump. A Teflon housing that fits the view cell was used to stabilize the MCs and the electromagnetic actuator which consisted of a coil made from Cu wire, as shown in Figure 2. The electrical connection for actuation in the pressure vessel was achieved by using insulated CONAX Technologies TG24T gland assemblies. All valves and connections were Swagelok . Throughout the operation, the temperature in the vessel was held constant by circulating fluid through tubing wrapped around the vessel using a Polyscience recirculator. AC actuation of 10 V was provided by Agilent 33220A Function Generator and the resonance spectrum obtained from LDV was amplified and filtered by Stanford Research SR560 Preamplifier and visualized by Tektronix TDS 654C Oscilloscope. The operation of the signal generator and the oscilloscope and the data acquisition were achieved using Instrument Control Toolbox in MATLAB via Keithley KUSB-488A GPIB-USB interface and the GPIB cable that connects the signal generator and the oscilloscope.

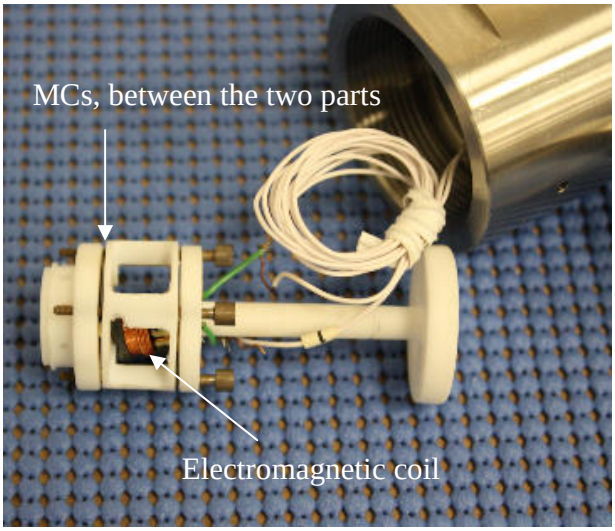

Figure 2: Custom-made Teflon housing for immobilization of MCs and electromagnetic coil

The overall experimental set-up is shown in Figure 3.

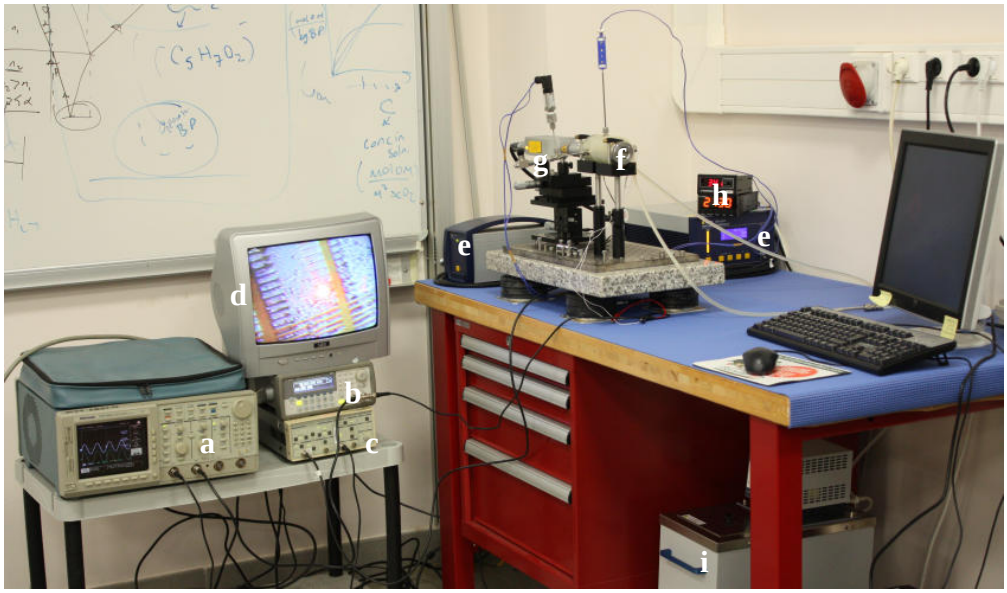

Figure 3: The experimental setup. (a) Oscilloscope (b) Signal Generator (c) Preamplifier (d) CRT TV (e) LDV control unit (f) Pressure Vessel (g) LDV laser unit (h) Temperature and Pressure Indicators (i) Recirculator

RESULTS

The representative experimental resonant spectra plots for both MCs (12x120x2.5 and 12x180x2.5) are shown in Figure 1. The overall experimental data are tabulated below.

Table 1: Overall experimental data of resonance spectra at different pressures for both cantilevers, sc: supercritical, g: gas

	12x120x2.5 (in µm)				12x180x2.5 (in µm)			
Phase	**P (psia)**	**T (ºC)**	**f_R (Hz)**	**Q**	**P (psia)**	**T (ºC)**	**f_R (Hz)**	**Q**
sc	1999	33.65	91280.56	16.89	1999	33.70	39163.00	11.00
sc	1824	33.60	92013.20	16.00	1820	33.60	39432.33	11.00
sc	1720	33.60	92266.00	17.00	1720	33.60	39653.00	11.80
sc	1620	33.70	93216.40	17.20	1620	33.70	39820.00	12.00
sc	1520	33.60	93482.33	17.00	1520	33.60	39887.00	12.00
sc	1420	33.60	94165.20	18.00	1420	33.60	40371.80	12.20
sc	1284	33.60	95222.00	19.53	1284	33.60	40857.00	19.50
g	984	33.70	102944.75	33.75	984	33.60	45477.40	25.00
air	14.7	33.63	119118.30	334.33	14.7	33.60	50658.50	89.00

Except for the last row where CO_2 is in gas phase, all other rows correspond to values obtained in supercritical phase. Between 984.70 psia and 1284.70 psia, no stable resonance spectra data could be obtained; for that reason, in the analysis only the supercritical phase values were used. This is possibly due to the divergence of density and viscosity and increasing substantial fluctuations in the medium in the proximity of the critical point.

The literature values of density and viscosity of CO_2 at the experimental points [19]are plotted in Figure 4.

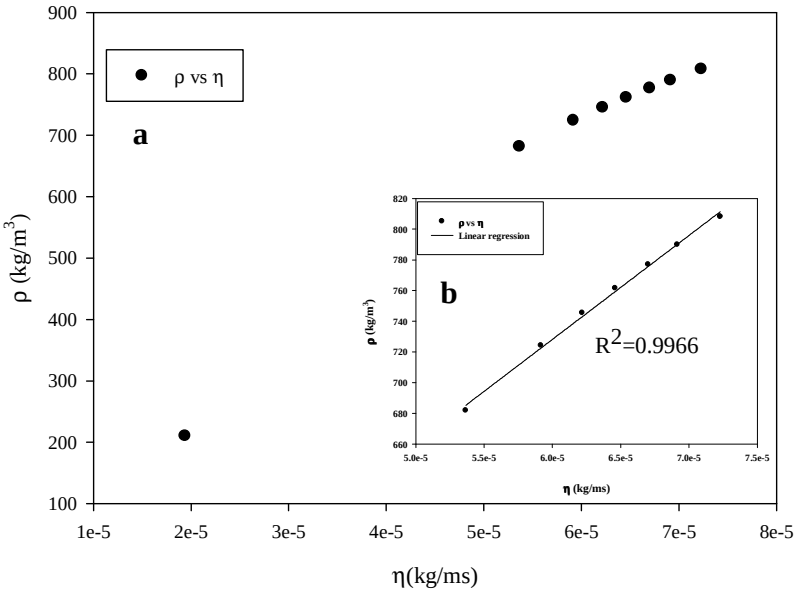

Figure 4: (a) Density versus viscosity plot for all experimental data points (gas and supercritical) (b) The linear fit to density versus viscosity plot only for data points in supercritical phase

It is observed that for the experimental pressure range, the variation of viscosity with density was almost linear. From the literature values, it can be also seen that both the density and viscosity increase linearly with increasing pressure. For that reason, the resonance frequencies of both cantilevers are plotted with respect to viscosity/density, i.e. kinematic viscosity, as seen in Figure 5.

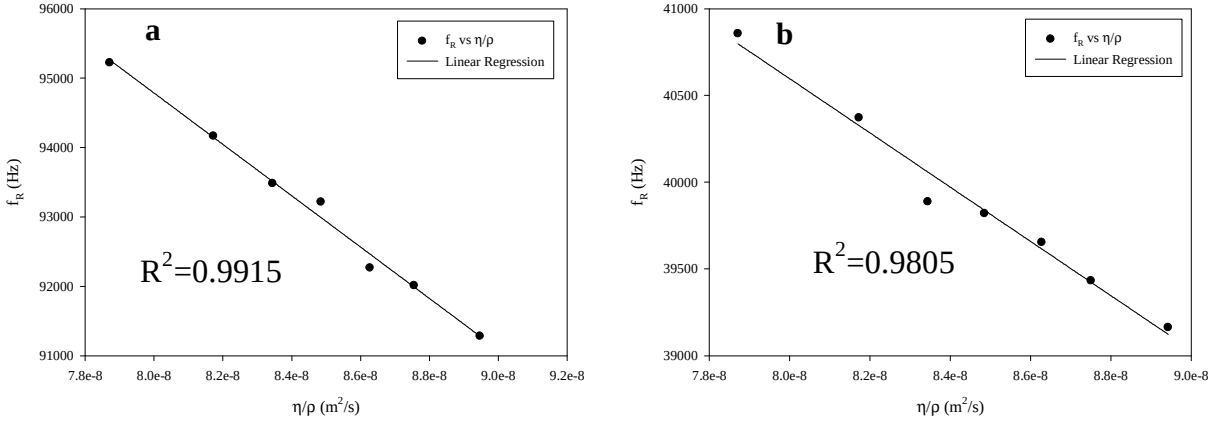

Figure 5: f_R (Hz) versus η/ρ (m^2/s) plots for cantilevers of size (a) 12x120x2.5 (b) 12x180x2.5

Figure 5 shows that there is almost a linear relationship between the resonance frequency and the kinematic viscosity for both cantilevers. This is possibly related to the specific combination of

the effects of density and viscosity on the hydrodynamic load experienced by the cantilevers. This result is independent of the length of the cantilevers, a phenomenon which is in agreement with the theoretical studies showing that the dominant length scale in the hydrodynamic flow is the width of the cantilevers [20].

The quality factor values of both cantilevers are also plotted with respect to kinematic viscosity, as seen in Figure 6.

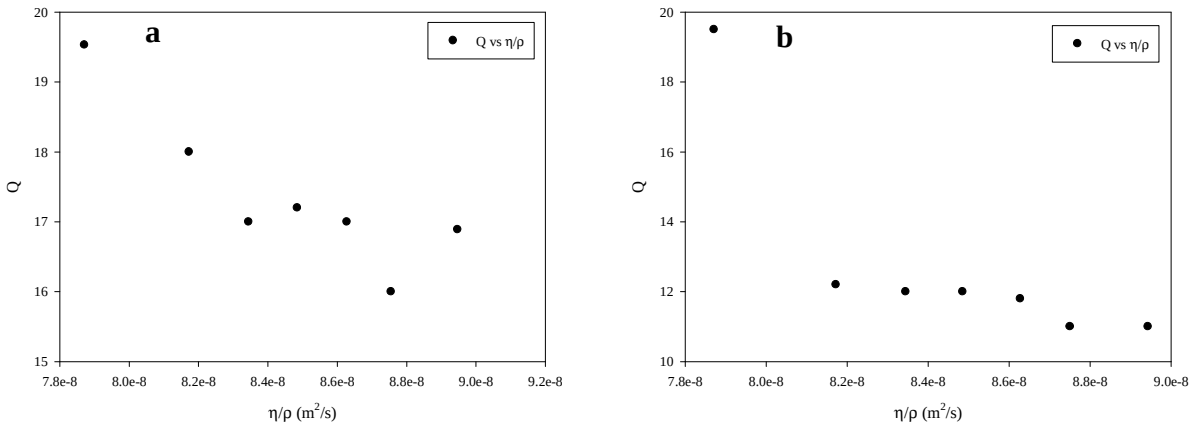

Figure 6: Q versus η/ρ (m^2/s) plots for cantilevers of size (a) 12x120x2.5 (b) 12x180x2.5

As shown in Figure 6, the relationship between the quality factor and the kinematic viscosity seems to have a highly nonlinear character. For the cantilever of size 12x120x2.5, the fluctuations are possibly due to the experimental errors. However, for both cantilevers it can safely be pointed out that the increase in kinematic viscosity results in decrease in quality factor.

In line with the added mass and damping effects explained in Introduction, both the resonance frequency and quality factor values decreases as pressure increases, as seen in Table 1. The shifts in resonance frequency are higher for the 120 μm long cantilever compared to those of the 180 μm long cantilever due to the fact that sensitivity due to added mass increases with decreasing length, which in turn corresponds to increasing resonance frequency. Therefore, it can be concluded that the MCs with higher resonance frequencies are more sensitive to added mass effects. This increase in sensitivity is obvious from the 1st order Taylor expansion of well-known resonance frequency expression written as a function of added mass [21]:

$$\frac{\Delta f}{f} \cong -\frac{1}{2}\frac{\Delta m}{m} \qquad (1)$$

In order to get a notion about the order of magnitude mass sensitivity of MCs under consideration, the added masses are calculated using Eq. 1 and plotted with respect to kinematic viscosity as seen in Figure 7.

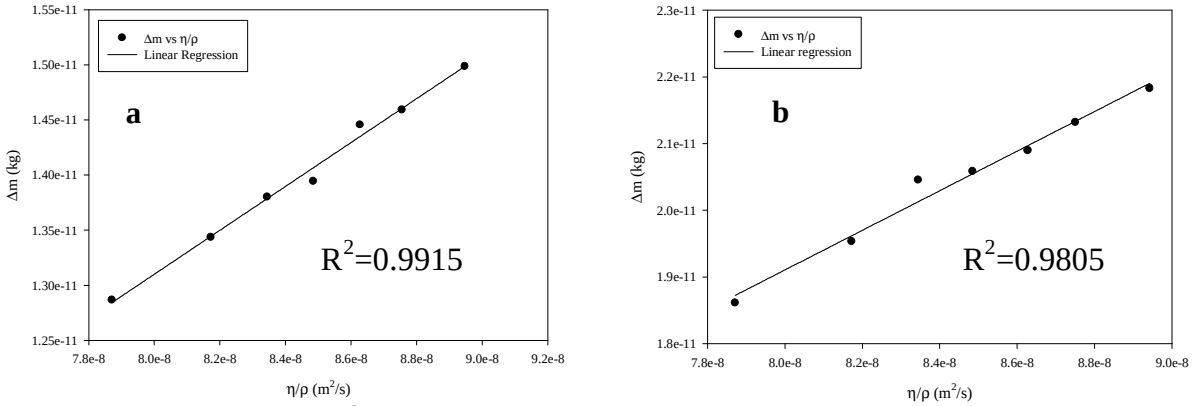

Figure 7: Δm (kg) versus η/ρ (m^2/s) plots for cantilevers of size (a) 12x120x2.5 (b) 12x180x2.5

It is seen that almost nanogram mass resolution can be theoretically achieved with the MCs under the stated conditions.

In addition, the extrapolation of resonance frequency versus density, viscosity (dynamic) and kinematic viscosity lines enabled us to calculate the resonance frequencies of MCs in air, values which are very close to vacuum frequency of MCs. This result is interesting and is not expected. Table 2 shows the percentage error in vacuum frequency calculation via extrapolation for both MCs.

Table 2: Percentage errors in vacuum frequency calculation by extrapolation

	12x120x2.5 (in μm)	12x180x2.5 (in μm)
f_R vs ρ	1.9	1.3
f_R vs η	10.3	9.8
f_R vs η/ρ	4.4	4.8

As depicted in Table 2, extrapolation of f_R versus ρ lines gives the best vacuum frequency values compared that of other lines. This is possibly due to closer relationship of density with added mass.

Finally, the relationship between the damping coefficient (β) and viscosity is investigated. A study showed that there is a quadratic relationship between the damping coefficient and viscosity [5] in the form:

$$\beta = C\eta^{1/2} \tag{2}$$

In Figure 8, the damping coefficients are plotted with respect to square root of viscosity for both MCs.

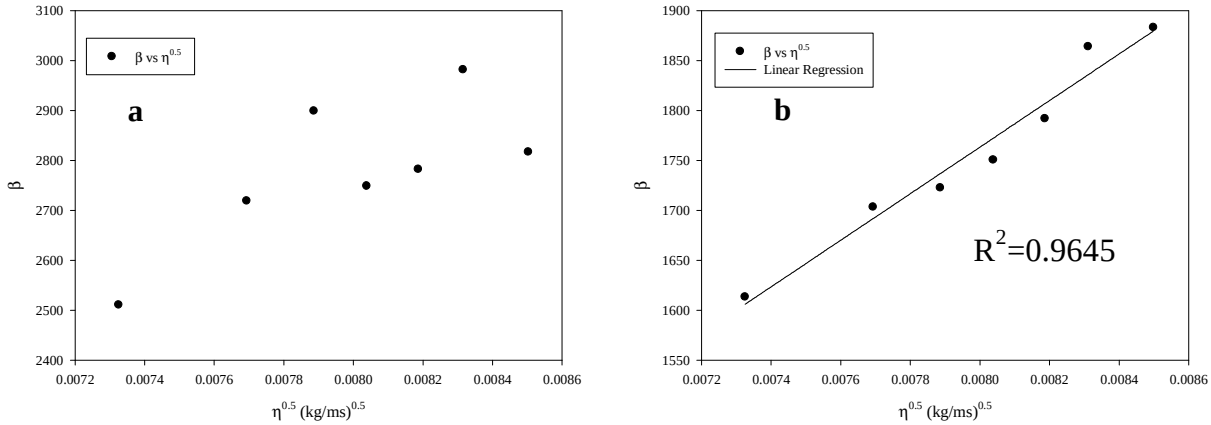

Figure 8: β versus $\eta^{0.5}$ plots for cantilevers of size (a) 12x120x2.5 (b) 12x180x2.5

As shown in Figure 8, it is not possible to extract a relationship between the damping coefficient and the square root of viscosity for cantilever of size 12x120x2.5 (in μm). The fluctuations are possibly due to experimental errors, a situation which is also obvious from the oscillatory behavior of quality factor in Figure 6 since it is well-known that damping coefficient is directly related to quality factor. However, for the other cantilever, a linear relationship between the damping coefficient and square root of viscosity is confirmed. Thus, this line can be used to calculate viscosity of $scCO_2$ with a percentage error less than 5% at the given conditions, which is fairly good for many applications. This procedure can also be combined with the linearity f_R versus η/ρ curves given in Figure 5 and density of $scCO_2$ can be calculated with a percentage error less than 3%.

CONCLUSION

In this study, the frequency response of MCs of sizes 12 μm x 120 μm x 2.5 μm and 12 μm x 180 μm x 2.5 μm in $scCO_2$ between 1200 psia and 2000 psia at 33.6 ºC is investigated. The analysis of the results showed that there is a linear relationship between the resonance frequency and kinematic viscosity. However, the behavior of quality factor with respect to kinematic viscosity is highly nonlinear. Added mass analysis shows that the mass resolution is on the order of nanograms for both cantilevers. Interestingly, it is shown that the vacuum frequency of the MCs can be calculated by the extrapolation of resonance frequency versus density lines with a percentage error less than 2 %. The quadratic relationship between the damping coefficient and viscosity is confirmed for the MC of length 180 μm. This result combined with the linear behavior of resonance frequency versus kinematic viscosity curves can be used to calculate the viscosity and density of $scCO_2$ with percentage errors less than 5 % and 3 %, respectively.

REFERENCES

[1] ILIC, B., CZAPLEWSKI, D., CRAIGHEAD, H. G., NEUZIL, P., CAMPAGNOLO, C., BATT, C., Applied Physics Letters, Vol. 77, **2000**, p. 450.
[2] MURALIDHARAN, G., WIG, A., PINNADUWAGE, L. A., HEDDEN, D., THUNDAT, T., LAREAU, R. T., Ultramicroscopy, Vol. 97, **2003**, p. 433.
[3] ONO, T., ESASHI, M., Review of Scientific Instruments, Vol. 74, **2003**, p. 5141.
[4] CHON, J. W. M., MULVANEY, P., SADER, J. E., Journal of Applied Physics, Vol. 87, **2000**, p. 3978.
[5] SCHILOWITZ, A. M., YABLON, D. G., LANSEY, E., ZYPMAN, F. R., Measurement, Vol. 41, **2008**, p. 1169.
[6] BOSKOVIC, S., CHON, J. W. M., MULVANEY, P., SADER, J. E., Journal of Rheology, Vol. 46, **2002**, p. 891.
[7] BELLON, L., Journal of Applied Physics, Vol. 104, **2008**.
[8] BELMILOUD, N., DUFOUR, I., NICU, L., COLIN, A., PISTRE, J., IEEE SENSORS 2006, EXCO, Daegu, Korea, Vol., **2006**, p. 753.
[9] HENNEMEYER, M., BURGHARDT, S., STARK, R. W., Sensors, Vol. 8, **2008**, p. 10.
[10] GOODWIN, A. R. H., DONZIER, E. P., VANCAUWENBERGHE, O., FITT, A. D., RONALDSON, K. A., WAKEHAM, W. A., DE LARA, M. M., MARTY, F., MERCIER, B., Journal of Chemical and Engineering Data, Vol. 51, **2006**, p. 190.
[11] ODEN, P. I., CHEN, G. Y., STEELE, R. A., WARMACK, R. J., THUNDAT, T., Applied Physics Letters, Vol. 68, **1996**, p. 3814.
[12] THUNDAT, T., ODEN, P. I., WARMACK, R. J., Microscale Thermophysical Engineering, Vol. 1, **1997**, p. 185.
[13] GOEDERS, K. M., COLTON, J. S., BOTTOMLEY, L. A., Chemical Reviews, Vol. 108, **2008**, p. 522.
[14] ROGERS, B., MANNING, L., JONES, M., SULCHEK, T., MURRAY, K., BENESCHOTT, B., ADAMS, J. D., HU, Z., THUNDAT, T., CAVAZOS, H., MINNE, S. C., Review of Scientific Instruments, Vol. 74, **2003**, p. 4899.
[15] FRANCA, D. R., BLOUIN, A., Measurement Science & Technology, Vol. 15, **2004**, p. 859.
[16] PASSIAN, A., WARMACK, R. J., WIG, A., FARAHI, R. H., MERIAUDEAU, F., FERRELL, T. L., THUNDAT, T., Ultramicroscopy, Vol. 97, **2003**, p. 401.
[17] VAN EYSDEN, C. A., SADER, J. E., Journal of Applied Physics, Vol. 100, **2006**.
[18] VAN EYSDEN, C. A., SADER, J. E., Journal of Applied Physics, Vol. 106, **2009**.
[19] NIST Chemistry WebBook, Thermophysical Properties of Fluid Systems, Vol. http://webbook.nist.gov/chemistry/fluid/.
[20] SADER, J. E., Journal of Applied Physics, Vol. 84, **1998**, p. 64.
[21] CIMALLA, V., NIEBELSCHUETZ, F., TONISCH, K., FOERSTER, C., BRUECKNER, K., CIMALLA, I., FRIEDRICH, T., PEZOLDT, J., STEPHAN, R., HEIN, M., AMBACHER, O., Sensors and Actuators B-Chemical, Vol. 126, **2007**, p. 24.